American Mineralogist, Volume 80, pages 520–533, 1995

Thermodynamic properties of stoichiometric staurolite $H_2Fe_4Al_{18}Si_8O_{48}$ and $H_6Fe_2Al_{18}Si_8O_{48}$

M. J. Holdaway, Biswajit Mukhopadhyay
Department of Geological Sciences, Southern Methodist University, Dallas, Texas 75275-0395, U.S.A.
B. L. Dutrow
Department of Geology and Geophysics, Louisiana State University, Baton Rouge, Louisiana 70803, U.S.A.

Abstract

Recent studies have shown that all natural and synthetic staurolite crystals are nonstoichiometric. In an Fe-Al-Si-O-H (FASH) system, the predominant hypothetical stoichiometric end-members are $H_2Fe_4Al_{18}Si_8O_{48}$ (2H) and $H_6Fe_2Al_{18}Si_8O_{48}$ (6H). End-member molar volume (V), specific heat (C_P), and calorimetric entropy (S) are presented on the basis of previous crystallographic and calorimetric work. Compositional data, including H content, are not available for any experimental staurolite. Because of the number of variables involved, it is necessary to use a trial and error approach to enthalpy (H) and entropy (S) retrieval. Using (1) the above values for V and C_P, (2) thermodynamic data for additional phases in the prograde staurolite + quartz reaction, (3) experimental data, including new data on the reaction of staurolite + quartz to sillimanite + almandine, (4) mole fraction models and composition estimates, and (5) natural data from Black Mountain, New Hampshire, and Maine, we have determined ΔH_f (-23961.25 ± 20 kJ/mol, -23992.86 ± 40 kJ/mol), S [918 ± 20 J/(mol·K), 850 ± 40 J/(mol·K)] for 2H and 6H staurolite. We have also determined H content in staurolite as a function of P, T, and coexisting phases. These values of S are substantially lower than corrected calorimetric values. These combined thermodynamic data for stoichiometric staurolite reproduce most of the experimental reversals, and show that synthetic and natural staurolite near staurolite + quartz breakdown conditions vary from H = 2.8 to >4.6 apfu with increasing P. Within the staurolite + quartz stability field, the composition of staurolite coexisting with almandine can be contoured for H content, which increases with P. Likewise, staurolite coexisting with aluminum silicate can be contoured for H content, which increases with P and decreases with T. For excess-SiO_2 rocks at any given P and T, the total range of FASH staurolite composition is between that which occurs with almandine and quartz and that which occurs with aluminum silicate and quartz. Those experimental data points that do not fit the calculated curve result mainly from use of H-poor staurolite as starting material under conditions at which H-rich staurolite is stable. Discrepancies between individual experimental data points and the curve calculated from the thermodynamic data are thus mainly the result of problems with experimental studies. These results provide an improved data set for calculation of staurolite equilibria.

Introduction

Staurolite is a common Al-, Fe-rich silicate in medium-grade pelitic schists. The crystal chemistry and thermodynamic properties of this mineral have long been an enigma because of incomplete understanding of its composition, crystal structure, and stoichiometry. In the last few years considerable progress has been made on several of the problems associated with staurolite. Lonker (1983) and Holdaway et al. (1986a) have shown that the H content of staurolite is variable; Dutrow et al. (1986) have shown that Li is an important constituent of many staurolite grains; Hawthorne et al. (1993a, 1993b, 1993c) have resolved most of the site-occupancy problems; Dyar et al. (1991) have contributed to our knowledge of the site occupancies and relative abundance of Fe^{2+} and Fe^{3+}; Holdaway et al. (1991) have provided methods of determining stoichiometry, site occupancies, and activity from chemical analyses.

Previous efforts at thermodynamic analysis of staurolite equilibria have not been very successful because of the incomplete understanding of the crystal chemistry of staurolite. Yardley (1981) obtained a thermodynamic fit of the experimental data of Ganguly (1972) and Rao and Johannes (1979) in the kyanite field and concluded that the correct formula has four H in the 48 O formula. However, Yardley was unable to fit most of the Richardson (1968) experiments in the sillimanite field. More recent experiments by Dutrow and Holdaway (1989) and Du-

0003–004X/95/0506–0520$02.00

trow (this report) in the sillimanite field are also inconsistent with Yardley's curve.

Pigage and Greenwood (1982) identified what seem to be the two main thermodynamic problems for staurolite: (1) The best thermodynamic fit to staurolite + quartz breakdown equilibria in the kyanite field is consistent with about four H in staurolite, whereas the best fit in the sillimanite field is consistent with about two H in staurolite (Pigage and Greenwood, 1982, Fig. 5). (2) Every thermodynamic analysis of staurolite experimental data indicates higher T or lower f_{H_2O} in rocks containing coexisting staurolite and breakdown products than is indicated by geothermobarometry of coexisting minerals. Holdaway et al. (1988) used this observation to suggest that staurolite solid solution at the T2 site is nonideal (site assignments are those of Hawthorne et al., 1993a).

In this report, we explain the problem related to the variable H content of staurolite. The relationship between composition and unit-cell constants in natural staurolite has enabled calculation of molar volumes of the stoichiometric Fe end-members (Holdaway et al., 1993). Specific heat (C_P), entropy (S), and enthalpy (H) for stoichiometric staurolite end-members with formulae $H_2Fe_4Al_{18}Si_8O_{48}$ (2H) and $H_6Fe_2Al_{18}Si_8O_{48}$ (6H) are presented. We caution that the thermodynamic data obtained depend on the model adopted to express thermodynamic concentration of the end-member components and are closely tied to the data used for aluminum silicate, almandine, quartz, and H_2O. In order to be appropriately applied, these data must be used in conjunction with the data used here for the additional minerals and with the same thermodynamic activity models. Alternatively, appropriate corrections must be made. An expanded version of the data, calculations, and additional notes is available as Table 1.[1]

Hypothetical stoichiometric end-member formulae

The most appropriate stoichiometric compositions for the two dominant staurolite end-members in the FeO-Al_2O_3-SiO_2-H_2O (FASH) system are designated 2H and 6H. Several other end-members also exist, even in the simple FASH system (Hawthorne et al., 1993c), but are treated here as diluting influences to the dominant end-members. Note that no natural or experimental staurolite actually approaches either end-member composition (Holdaway et al., 1991, 1993). We emphasize that any method for determining such staurolite end-members must involve assumptions because the combination of substitutions tends to defy quantification. A general formula for staurolite is $H_{2-8}(Fe^{2+},Mg,Zn,Li,Mn,Al,Fe^{3+},\square)_4^{T2}(Al,Mg,Fe^{2+})_8^{M1}(Al,Mg,Fe^{2+},Ti)_8^{M2}(Al,Mg,Fe^{2+},\square)_4^{M3}(\square,Fe^{2+},Zn,Li)_4^{M4}(Si,Al)_8^{T1}O_{48}$ (Holdaway et al., 1991; Henderson et al., 1993; Hawthorne et al., 1993a). Stoichiometric end-member compositions are chosen to minimize disorder. At high T, staurolite is either orthorhombic or very nearly so (Hawthorne et al., 1993b). For stoichiometric end-members, the following observations can be made: (1) The T2 site (multiplicity 4) is either filled with Fe^{2+} (in 2H) or vacant (in 6H staurolite). (2) The M1 and M2 sites (each of multiplicity 8) are filled with Al. (3) The M3 site (multiplicity 4) is 50% occupied by Al and is considered to have an effective multiplicity of 2. Although at low T, the M3 site is split into crystallographically distinct M3A and M3B sites with short-range Al-□ order, at crystallization T, as the structure becomes orthorhombic, M3A and M3B become equivalent and Al-□ disorder becomes complete (Hawthorne et al., 1993b). (4) The T1 site (multiplicity 8) is filled with Si. (5) The M4 site (multiplicity 4) is vacant in 2H staurolite and is 50% occupied with Fe^{2+} in 6H staurolite. At low T, M4 has short-range Fe-□ order, but at T of crystallization it is disordered (Hawthorne et al., 1993b). (6) The H1 site (multiplicity 4) is 50% occupied in both end-members giving an effective multiplicity of 2. (7) The H2 site (multiplicity 4) is either empty (in 2H) or full (in 6H staurolite). This stated multiplicity of 4 is half of the actual H2 multiplicity; the other half of the H2 positions are empty in 6H staurolite because of occupancy of the adjacent M4 sites to which H2 vacancies are coupled. H2 can only be occupied when both of the adjacent T2 and M4 sites are empty (Hawthorne et al., 1993c). Because of this local coupling, H2 has no independent disorder.

Disorder in stoichiometric end-member staurolite involves H1 linked alternatively to opposite ends of empty M3 octahedra in both end-members, Al-□ disorder in M3 in both end-members, and Fe-□ disorder in M4 of 6H staurolite. With the above constraints in mind, the two dominant FASH stoichiometric Fe^{2+} end-members are 2H Fe staurolite, $H_2Fe_4^{T2}Al_8^{M1}Al_8^{M2}Al_2^{M3}Si_8^{T1}O_{48} = H_2Fe_4Al_{18}Si_8O_{48}$ and 6H Fe staurolite, $H_6Fe_2^{M4}Al_8^{M1}Al_8^{M2}Al_2^{M3}Si_8^{T1}O_{48} = H_6Fe_2Al_{18}Si_8O_{48}$. In these end-members, all Al is octahedral, all Si is tetrahedral, Fe in 2H staurolite is tetrahedral, and Fe in 6H staurolite is octahedral.

Molar volume of stoichiometric end-members

The molar volumes (V) for these end-members (Table 2) result from multiple linear regression (Holdaway et al., 1993) of 22 staurolite compositions typical of medium-grade pelites. Although they may not accurately represent end-member values, they are suitable for retrieving thermodynamic data from (nonstoichiometric) synthetic or natural compositions and for applying thermodynamic data to staurolite. That is, they are partial molar volumes of common staurolite compositions. Their utility decreases for extreme or unusual staurolite compositions, especially Mg-rich varieties with >50 mol% Mg/(Mg + Fe). This is because such compositions are outside the range used for regression by Holdaway et al. (1993), and in Mg-

[1] A copy of Table 1 may be ordered as Document AM-95-589 from the Business Office, Mineralogical Society of America, 1130 Seventeenth Street NW, Suite 330, Washington, DC 20036, U.S.A. Please remit $5.00 in advance for the microfiche. Alternatively, contact M.J.H. directly.

TABLE 2. Recommended values of thermodynamic properties of 2H and 6H stoichiometric staurolite*

	2H	6H
V (J/bar)	44.610	44.165
a**	2897.922	2879.653
b	−0.004 079 9	−0.002 341 9
c	−6 270 828	−9 897 328
d	−27377.75	−25507.13
e	0.453×10^{-6}	0.453×10^{-6}
H (kJ/mol)	−23961.25 ± 20	−23992.86 ± 40
S [J/(mol·K)]	918 ± 20	850 ± 40

* See text for sources of data.
** $C_P = a + bT + cT^{-2} + dT^{-½} + eT^2$.

rich staurolite Mg occurs at M4, which does not contain Mg in more common Fe-rich staurolite (Hawthorne et al., 1993a).

SPECIFIC HEAT OF STOICHIOMETRIC END-MEMBERS

For C_P and for S (below), a structural analogue is required to adjust calorimetric values for staurolite to those of the stoichiometric FASH end-members. Specimen 355-1 (Zen, 1981; used by Hemingway and Robie, 1984, for C_P and S) has the formula $H_{3.317}Fe^{2+}_{3.239}Mg_{0.458}Mn_{0.028}Zn_{0.052}Li_{0.326}Co_{0.007}Al_{17.741}Fe^{3+}_{0.117}Cr_{0.013}V_{0.006}Si_{7.706}Ti_{0.084}O_{48}$ (Holdaway et al., 1986b, assuming 3.5% of Fe is Fe^{3+}; Dyar et al., 1991; Holdaway et al., 1991). The effects of non-FASH components on C_P were corrected by subtracting appropriate amounts of the C_P expression for each non-FASH oxide (MgO, MnO, ZnO, Li_2O, etc.) from an algebraic fit to Hemingway and Robie's (1984) C_P values for Zen's (1981) specimen 355-1. In order to adjust the resulting nonstoichiometric FASH C_P expression for the H, Fe, Al, and Si content of the two stoichiometric end-member formulas, the following sequence of steps was taken for each end-member: (1) Add or subtract the C_P expression of pyrophyllite to produce the correct H, and adjust Al and Si accordingly; (2) add or subtract C_P of fayalite to produce the correct Fe^{2+}, and adjust Si accordingly; (3) add or subtract C_P of kyanite to produce the correct Al, and adjust Si accordingly; (4) add or subtract C_P of low quartz to produce the correct Si. The resultant C_P expressions, applicable between 298 and 900 K, are given in Table 2. C_P curves for these end-members and for the original Hemingway and Robie (1984) determination are shown in Figure 1. The strengths of this structural analogue are that kyanite has a structure similar to the aluminum silicate layer of staurolite, and the coordination numbers of most of the oxides used for correction are the same as in staurolite. The weaknesses are: (1) Pyrophyllite is a poor model for H in staurolite, although we can think of no better model; (2) fayalite, with $^{[6]}Fe$, is used to model a chemical octahedral-tetrahedral substitution of Fe in staurolite. These problems are not expected to significantly affect the C_P expression above 298 K, but they will affect standard (298 K) entropies of the end-members discussed below. Two structural analogues used by Hemingway and Robie (1984) diverge significantly from measured values for staurolite below about 300 K but agree above that T. Similarly, C_P curves for dimorphs or for reactants and products of solid-solid reactions are comparable above 298 K but diverge significantly at lower T.

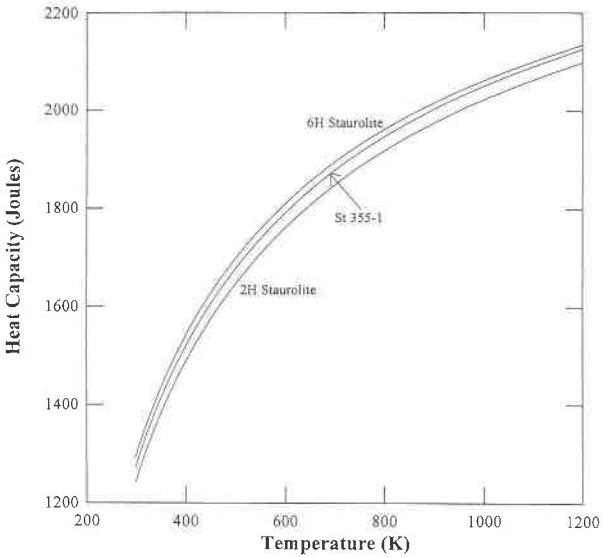

Fig. 1. Specific heat curves for staurolite. Specimen 355-1 is the staurolite determined by Hemingway and Robie (1984). The lowest curve is for stoichiometric 2H staurolite and the highest curve is for stoichiometric 6H staurolite (Table 2) determined with chemical corrections of the Hemingway and Robie (1984) C_P.

CALORIMETRIC ENTROPY OF STOICHIOMETRIC END-MEMBERS

The entropy of stoichiometric staurolite may be estimated in two ways: by use of a structural analogue applied to the calorimetric data and by retrieval of S from experimental stability results. Partly because of the weaknesses of the structural analogue required for the calorimetric method, the resultant values of S are not of good quality, especially for the 6H end-member for which significant extrapolations are involved for H and Fe.

Specimen 355-1 was used as a starting point because Hemingway and Robie (1984) provided complete C_P data. To evaluate S of the stoichiometric end-members, we began with a staurolite S value having no corrections. Entropy of 355-1 at 298 K without chemical or disorder corrections is 1101.0 (calorimetric S, including a chemical correction) minus 121.0 (chemical correction), which equals 980.0 J/(mol·K) (Hemingway and Robie, 1984, Table 6). However, corrections to this value are required for the specific chemical, volume, and disorder effects of our end-member staurolite. Chemical corrections were made using the structural analogue described previously.

Volume corrections were made by comparing the molar volume of the end-member staurolite (above) with the molar volume calculated for specimen 355-1 (Holdaway et al., 1993) algebraically combined with the molar vol-

umes of the structural analogue components. The correction factor of 20.92 J/(mol·K) for each J/bar of volume (Fyfe et al., 1958) was used to correct S for volume effects. Staurolite with two H has a volume that is 0.499 J/bar lower than that calculated from specimen 355-1 and the structural analogue, resulting in a subtraction of 10.4 J/(mol·K); staurolite with six H has 1.211 J/bar more volume than that calculated, equaling an addition of 25.3 J/(mol·K).

Disorder corrections are needed for sites H1 and M3 in both staurolite end-members and for site M4 in 6H staurolite. For the H1 site, the disorder can be viewed as 50% of one configuration about an empty M3 octahedron (H-□) and 50% of the alternative configuration (□-H). There are a total of two cation-vacancy pairs. H1 disorder S becomes $-2(X_1 \ln X_1 + X_2 \ln X_2)$ or $-2(0.5 \ln 0.5 + 0.5 \ln 0.5) = 11.53$ J/(mol·K). For both M3 and M4 we assume complete cation-vacancy disorder. For two cations and two vacancies distributed randomly over four sites, S disorder becomes $-4(0.5 \ln 0.5 + 0.5 \ln 0.5) = 23.06$ J/(mol·K). Thus, the 2H end-member has 34.6 and the 6H end-member has 57.7 J/(mol·K) disorder S. Because this model assumes a fully disordered orthorhombic staurolite, it gives an upper limit of possible configurational entropy.

All the corrections and the final S values are given in Table 3. Standard deviations are estimated as the root-mean-square combination of the calorimetric error [12 J/(mol·K)], 50% of the volume correction, 50% of the chemical correction, and 50% of the disorder correction. As shown below, these entropies are significantly higher than those retrieved from experimental reversals and probably should not be used.

TABLE 3. Corrected calorimetric entropy in J/(mol·K) for stoichiometric 2H and 6H staurolite

	2H	6H
355-1	980.0	980.0
Chemical	−12.6	−4.2
V	−10.4	+25.3
Disorder	+34.6	+57.7
Total	991.6	1058.8
Error (σ)	±22.6	±33.8

Note: these values are substantially higher than entropies retrieved from experimental studies (Table 2).

RETRIEVAL OF ENTROPY AND ENTHALPY FROM EXPERIMENTAL RESULTS AND NATURAL OCCURRENCES

New experiments

New results on the metastable extension of the reaction of staurolite + quartz to almandine + sillimanite (Reaction 2 below) were completed by B.L.D. In order for the high-P experiments to be compatible with those done at lower P, starting materials were identical to those of Dutrow and Holdaway (1989): natural Fe-rich staurolite, sample 78332, $H_{3.272}Fe^{2+}_{3.214}Mg_{0.639}Mn_{0.019}Zn_{0.023}Li_{0.124}Co_{0.004}Al_{17.783}Fe^{3+}_{0.117}Cr_{0.016}V_{0.007}Si_{7.667}Ti_{0.103}O_{48}$ (Holdaway et al., 1986b, 1991); quartz from Hot Springs, Arkansas; fibrolite-free sillimanite from Montville Quadrangle, Connecticut (Holdaway, 1971); and almandine synthesized at 800 °C, 10 kbar. Because of the recalcitrant nature of the phases, aliquots of all minerals participating in the reaction plus H_2O were initially present in the capsule. For each experiment, the starting solids consisted of 5% staurolite seeds and about 32% each of quartz, sillimanite, and almandine.

A double-capsule technique was used to maintain the oxidation state of Fe. Approximately 20 mg of the mixture was packed with H_2O into an inner AgPd capsule (ca. 4 mm long, 1 mm o.d.), sealed, placed within a Au capsule (ca. 8 mm long), and surrounded by powder of quartz-fayalite-magnetite (QFM) and sufficient H_2O to define f_{O_2} conditions equivalent to the QFM buffer (Eugster and Wones, 1962). This technique assured that most Fe remained in the divalent state.

Isobaric experiments were done with a piston-cylinder apparatus at 9 and 14 kbar. P and T were automatically regulated to within ±1%. Durations of experiments were 7–14 d at 14 kbar and 14 d at 9 kbar. Sample assemblies were surrounded by an outer NaCl cell around a graphite furnace. Within the furnace, a fired pyrophyllite cylinder was above the capsule and a NaCl filter-plug below the capsule. The capsule was encased in a fired pyrophyllite sheath and separated from the NaCl filters and pyrophyllite cylinder by a 0.3-mm-thick pyrophyllite plate. The top plate also served to isolate the chromel-alumel thermocouple from the metal capsule. The complete assembly was coated with Mo and wrapped in Pb foil. A symmetric T distribution was assumed within the capsule and the capsule's center was placed at T_{max} (in length) within the furnace. Postexperiment measurements of the capsules were made to determine length change owing to loading and T was corrected accordingly. Thermocouple-emf readings were corrected for P according to Getting and Kennedy (1970). After each experiment, both buffer and experimental products were examined for H_2O, and the buffer was examined optically to insure that QFM f_{O_2} conditions were maintained.

Experimental products were examined with a SEM and by XRD. Direction of reaction was primarily based on staurolite textures because of the small amount of reaction. Textural criteria for determining staurolite growth and dissolution were those described by Dutrow and Holdaway (1989). At 9 kbar, staurolite grew at 700 °C and broke down at 715 °C. At 14 kbar, staurolite grew at 720 °C and broke down at 750 °C. These conditions, extended in T and P as discussed below, are included in the data used for retrieval of H and S. At 14 kbar and 700 °C, euhedral staurolite crystals were observed in the experiment products.

Nature of experimental reversals for staurolite

In a strict sense, no experiments on staurolite stability are true reversals. For experiments that involved synthetic

FASH staurolite as the starting material (Ganguly, 1972; Rao and Johannes, 1979; Richardson, 1968), one cannot be sure that the Fe-H ratio of the starting staurolite was near the equilibrium value, and one must hope that the synthesized mineral equilibrated in composition before reacting. For experiments that involved natural staurolite (Dutrow and Holdaway, 1989; this report) one can (accidentally) choose a staurolite with about the correct H content, but all natural staurolite contains impurities such as Mg, Mn, Zn, Li, and Ti. In these experiments, the effects of impurities were minimized by three factors. First, the natural staurolite used in these experiments had very little Mn, Zn, Li, and Ti (each 0.4–3% of the non-Si, Al cations, see formula above). Because Fe and Mg partition rather evenly between product garnet and reactant staurolite, the effect of about 17 mol% Mg/(Mg + Fe) in the staurolite seeds is only a few degrees Celsius. Thus the staurolite reacted at conditions close to those of pure Fe staurolite. Second, in all experiments of Dutrow and Holdaway (1989) and this report, the natural staurolite used was present in seed amounts only. Thus, there was a tendency for the rims of staurolite seeds to change composition by ion exchange with the surrounding Fe-rich environment. Third, as stable staurolite grew, it became enriched in the FASH components that were the only constituents of the surrounding minerals.

Despite these factors, we conclude that the most significant experiments are those in which staurolite grew. An experiment that produced breakdown products or showed staurolite reaction might represent a case where a slightly unstable staurolite reacted to breakdown products just inside the stability field of a different stable FASH staurolite composition. Alternatively, such experiments might not produce enough change to demonstrate reaction.

To date, experimental staurolite product compositions have not been measured in any of the various studies. As will be shown below, reasonable assumptions must be made regarding staurolite composition. The composition of the staurolite starting mix cannot be expected to reflect its final composition because staurolite compositions vary with the experimental P and T and with coexisting phases such as garnet or aluminum silicate.

Activity models

For the calculations given below, it is necessary for us to have activity models that can be applied to both synthetic and natural staurolite. We assume that synthetic staurolite forms on a solid-solution series between $H_{2.8}Fe^{2+}_{4.45}Al_{17.80}Fe^{3+}_{0.10}Si_{7.65}O_{48}$ and $H_{6.8}Fe^{2+}_{2.45}Al_{17.80}Fe^{3+}_{0.10}Si_{7.65}O_{48}$. These formulae are chemical end-members and represent the Fe^{2+}-H substitution in FASH staurolite calculated from the average compositions of natural staurolite occurring with quartz (Holdaway et al., 1991). They represent the 2H and 6H end-members combined with additional substitutions in every site of the staurolite structure. Synthetic staurolite cannot be stoichiometric and has simple whole number coefficients. When multiple linear-regression constants derived from molar volumes of natural staurolite are applied to synthetic FASH staurolite with an assumed stoichiometric ratio of $Fe_4Al_{18}Si_8$, measured unit-cell volumes require H contents significantly <2. On the other hand, if synthetic FASH staurolite is assumed to have compositions on the series given above, unit-cell volumes predict reasonable H contents (Holdaway et al., 1993). Thus, an activity model must be used to retrieve thermodynamic data even in the synthetic system.

Staurolite stoichiometry is based on 48 O. For natural staurolite that formed under reducing conditions and for which Fe^{3+} is unknown, we assume 3.5% of Fe is Fe^{3+} (Holdaway et al., 1991). For synthetic staurolite that formed under conditions at or near the QFM buffer, we assume 0.1 Fe^{3+} apfu. Minor Fe^{3+} has no significant effect on the mole fraction as it apparently substitutes for Al at T2 (Holdaway et al., 1991), which is nominally occupied by Fe^{2+} in 2H or is vacant in 6H Fe staurolite.

The procedure used for cation assignment in natural and synthetic staurolite is slightly modified from that given by Holdaway et al. (1991, p. 1915) by the results of Henderson et al. (1993) in which Ti is assigned to M2 instead of T2. Minor improvements in the revised data set of Hawthorne et al. (1993a) have also been incorporated. For these calculations, we assumed that occupancies of M3 and M4 vary between 0 and 2 and ignored the additional two vacancies in each site. The modified assignment procedure becomes: (1) Subtract the total number of (non-H) cations from 30. This number is equal to $^{T2}\square + {}^{M3}\square - {}^{M4}$occupancy. Assign vacancies so that occupancy at normally vacant M4 equals half of the vacancy at T2, $^{T2}\square = 2(2 - {}^{M4}\square)$, and vacancy at M3 is determined by $K_D = 1.1 = {}^{T2}[(\square/2)/(4 - \square)]\cdot{}^{M3}[(2 - \square)/\square]$. This is based on three crystal-structure refinements of compositionally normal H-rich staurolite (Hawthorne et al., 1993a) in which $^{T2}\square$ is about four times $^{M3}\square$. Vacancies at T2 must occur in pairs because they are coupled in pairs to individual occupancy of M4. (2) Assign (Fe^{2+} + Mg) totaling 0.30 to M1, assign all Ti plus necessary (Fe^{2+} + Mg) totaling 0.21 to M2, 0.12 (Fe^{2+} + Mg) to M3, and the remaining (Fe^{2+} + Mg) provisionally to T2. (3) Assign Al as 7.70 to M1, 7.79 to M2, the amount needed to M3, (8 − Si) to T1, and the remainder to T2. (4) Assign all Zn, Li, Fe^{3+}, and Mn provisionally to T2. (5) Fill the previously determined occupancy of M4 with Fe^{2+} + Zn + Li from T2 so that they partition equally between T2 and M4; that is, ^{T2}(Li/Fe) = ^{M4}(Li/Fe), and ^{T2}(Zn/Fe) = ^{M4}(Zn/Fe). (6) Partition all Mg and Fe^{2+} (excluding Fe^{2+} in M4) between T2 and M1-M3 using partition coefficients: $^{T2}(Fe^{2+}/Mg)\cdot{}^{x}(Mg/Fe^{2+}) = 14.04$, 6.26, and 32.4, where x = M1, M2, and M3, respectively. Steps 5 and 6 require several iterations and are best done with tentative T2 and M4 assignments followed by tentative M1 and M3 assignments in order, and finally T2 and M4 are recalculated. The iterations are most easily done by comparison with an already determined staurolite stoichiometry. (Note that Mg-rich staurolite could be accommodated by partition-

ing Fe strongly into M4 relative to Mg. The present approach excludes Mg-rich staurolite, which has Mg in M4.)

Our activity models represent a compromise between the oversimplified models used in most studies of staurolite reactions and the high degree of complexity indicated by the results of Hawthorne et al. (1993a, 1993b, 1993c). In their work they demonstrate that even in simple systems there is predictable solid solution on every single site of staurolite. Holdaway et al. (1991) have adapted the site occupancies of Hawthorne et al. (1993a) to a simple FASH system. These site occupancies should be applicable to synthetic staurolite and should produce better compositions than any other presently available approach. For activity models, we use the general approach that, with the exception of two H at H1 in each end-member, all H variation and location is specifically coupled to other substitutions at T1, T2, and M1-M4 to satisfy local charge-balance requirements. Therefore, H is unnecessary in mole-fraction models. The 2H staurolite mole-fraction model is modified from Holdaway et al. (1991) to be consistent with the 6H model given below. The Al occupancy for M1 and M2 is taken from the cation assignment procedure discussed above, which in turn results from the average Al of the Hawthorne et al. (1993a) cation occupancies. For sites such as M3 and M4 in which 50% vacancy solid solution occurs in one or more end-members, a normalization procedure is required (Spear, 1993, p. 183). However, when the vacancy half of the site is always empty, as with staurolite, this reduces to ${}^{M3}X^{2}_{Al}$ with X_{Al} taken as mole fraction of the half site (Al/2).

For both the 2H and 6H end-members, vacancy-occupancy substitutions in either M4 or T2, but not both, must be accounted for because of coupling. Hawthorne et al. (1993c) have shown that adjacent occupancy of M4 and T2 by any cations is impossible because the M4-T2 distance is only 1.64 Å across a shared face. We choose the M4 site to model the vacancy-occupancy substitution for both end-members because the T2 vacancies must occur in pairs (Hawthorne et al., 1993c) coupled to M4 occupancy. In the ideal case, the M4 mole fraction models both dilution of M4 by other ions and the coupled substitution with T2. This is analogous to a system with three components: ${}^{M4}Fe_2\,{}^{T2}\square_4H_4$, ${}^{M4}Zn_2\,{}^{T2}\square_4H_4$, and ${}^{M4}\square_2\,{}^{T2}Fe_4\square_4$. The first applies to 6H staurolite and the third to 2H staurolite. For the 2H staurolite end-member, an additional factor is needed to account for dilution of occupied T2 by ions other than Fe^{2+}. The Hawthorne et al. (1993a) site occupancies show that in H-rich staurolite M3 has less Al while T2 has more Al, by about the same amount. Therefore, we assume that these two Al substitutions are coupled and should be modeled only by M3 Al mole fraction. Dilution of Fe^{2+} in T2 is thus modeled on the basis of $(4 - {}^{T2}\square - {}^{M3}\square) = n$ cations. The T2 factor for 2H staurolite equals one in hypothetical stoichiometric 2H-6H staurolite solid solutions and is essentially constant at 0.83 in synthetic FASH staurolite. This factor is not needed in the 6H staurolite activity model because there is no Fe^{2+} at the T2 site in the 6H formula to be diluted by other cations. The activity model for 2H stoichiometric staurolite is

$$X^{St}_{2HFe\text{-}St} = {}^{M1}\left(\tfrac{7.70}{8}\right)^{8} \cdot {}^{M2}\left(\tfrac{7.79}{8}\right)^{8} \cdot {}^{M3}X^{2}_{Al} \cdot {}^{T1}X^{8}_{Si} \cdot {}^{M4}X^{2}_{\square} \cdot {}^{T2}X^{n}_{Fe^{2+}}$$

$$= 0.5954\,{}^{M3}X^{2}_{Al} \cdot {}^{T1}X^{8}_{Si} \cdot {}^{M4}X^{2}_{\square} \cdot {}^{T2}X^{n}_{Fe^{2+}}$$

where ${}^{T2}X_{Fe^{2+}} = {}^{T2}Fe^{2+}/n$. The activity model for 6H stoichiometric staurolite is

$$X^{St}_{6HFe\text{-}St} = {}^{M1}\left(\tfrac{7.70}{8}\right)^{8} \cdot {}^{M2}\left(\tfrac{7.79}{8}\right)^{8} \cdot {}^{M3}X^{2}_{Al} \cdot {}^{T1}X^{8}_{Si} \cdot {}^{M4}X^{2}_{Fe^{2+}}$$

$$= 0.5954\,{}^{M3}X^{2}_{Al} \cdot {}^{T1}X^{8}_{Si} \cdot {}^{M4}X^{2}_{Fe^{2+}}.$$

Some questions regarding these activity models have been raised by reviewers. Although the models proposed here may not be theoretically perfect, we believe they are the best that can be done at this time. One question involves whether a single site, M4, can be used to model adequately the vacancy-occupancy substitution between M4, T2, and H sites. The case here for coupling between these sites is considerably stronger than for minerals like plagioclase because Hawthorne et al. (1993c) have shown that adjacent M4 and T2 sites cannot both be occupied. It is our assumption that H^+ ions simply occupy positions as required for local charge balance (Holdaway et al., 1991). A related question is whether these models reduce to simple mole fractions (or powers of mole fractions) of the components in a purely two-component system. In the fictitious stoichiometric two-component FASH system with only Fe^{2+}-H substitution and all Al and Si sites occupied by Al and Si, respectively, the 2H staurolite activity model reduces to ${}^{M4}X^{2}_{\square}$ and the 6H staurolite activity model reduces to ${}^{M4}X^{2}_{Fe^{2+}}$, all other factors being one. If additional components are added, ${}^{M4}X^{2}_{Fe^{2+}}$ models both the vacancy-occupancy substitution and the dilution of Fe^{2+} in M4 by other ions, a small effect at M4 as seen from the results of Hawthorne et al. (1993a). This is analogous to the ideal activity of albite X_{Na} in a ternary feldspar being partly the result of dilution by anorthite and the associated coupling ion and partly the result of dilution by orthoclase without any coupling. The ${}^{T2}X^{n}_{Fe^{2+}}$ factor in 2H staurolite results solely from additional components and is one in a fictitious stoichiometric FASH staurolite with only Fe^{2+}-H substitution. This factor does not enter into the 6H end-member activity because its formula contains a vacancy at T2, which in turn is coupled to M4 occupancy.

Initially, we assumed that staurolite solid solution at each site is ideal. For the 2H-6H staurolite solid solution, slight error in this assumption would tend to modify the retrieved H and S values in such a way as to offset inaccuracy introduced by assuming ideality in the compositional range of common and synthetic staurolite. For the cations that collectively substitute at T2, activities of natural 2H staurolite were determined both with and without a +9 kJ/ion symmetrical Margules parameter (Mukhopadhyay et al., 1990) for Fe^{2+} vs. (Mg + Zn + Li + Mn) at T2. The correction for T2 nonideality has a very small effect on the calculated results but allows for a slightly more reasonable S of 6H staurolite and a better overall

TABLE 4. Calculated activities of 2H and 6H staurolite and almandine

H sample	$X^{St}_{2H\ Fe\text{-}St}$	$a^{St}_{2H\ Fe\text{-}St}$*	$a^{St}_{6H\ Fe\text{-}St}$	X^{Gt}_{Alm}**
		Synthetic		
2.8	0.3060	0.3060	0	1
3.0	0.2758	0.2758	0.000416	1
3.2	0.2479	0.2479	0.00159	1
3.4	0.2221	0.2221	0.00341	1
3.6	0.1982	0.1982	0.00573	1
3.8	0.1763	0.1763	0.00849	1
4.0	0.1562	0.1562	0.0116	1
4.2	0.1378	0.1378	0.0148	1
4.4	0.1210	0.1210	0.0183	1
4.6	0.1059	0.1059	0.0217	1
		Black Mountain (≥495 °C, 5.5 kbar, H = 3.99–4.56 apfu)		
71-62U	0.0273	0.0320	0.0136	—
71-62T	0.0268	0.0314	0.0159	—
71-62B	0.0303	0.0356	0.0131	—
Av.	0.0281(19)	0.0330(23)	0.0142(15)	—
		Maine M_3 (~540 °C, 3.1 kbar, H = 2.97–3.27 apfu)†		
3-3	0.1177	0.1510	0.00038	0.3285
86	0.1291	0.1656	0.00028	0.5514
114-1	0.1172	0.1503	0.00009	0.5354
164	0.1152	0.1478	0.00133	0.4253
53-2	0.1140	0.1462	0.00029	0.4495
Av.	0.1186(60)	0.1522(77)	0.00047(49)	0.4580(903)

Note: where an H content (in apfu) is given, calculated activities are for synthetic staurolite of compositions assumed in text. Where a locality and sample number are given, calculated activities are for natural staurolite and garnet, where present.

* Based on 9 kJ per T2 site (Mukhopadhyay et al., 1990).

** Garnet activity corrections were not necessary because of the uncertain value of $a^{St}_{6H\ Fe\text{-}St}$.

† H contents of the Maine staurolite have been increased by 0.3 apfu to provide better agreement with the structure analysis of Hawthorne et al. (1993a). The discrepancy probably results from higher quartz inclusion content than that of other staurolite samples analyzed by Holdaway et al. (1986a). Resulting values of $a^{St}_{6H\ Fe\text{-}St}$ have at least 50% error.

fit on the basis of natural constraints. Table 4 gives the activities of 2H and 6H staurolite for synthetic staurolite at 0.2 apfu intervals of H content, for natural staurolite from Black Mountain, New Hampshire (Rumble, 1978), and for natural staurolite and garnet from Maine M_3 (Holdaway et al., 1988). Staurolite analyses for these rocks are from Holdaway et al. (1986b) and Dyar et al. (1991).

Equilibria

For the purpose of retrieval of thermodynamic data for staurolite, we consider only those equilibria involving various combinations of 2H-6H staurolite solid solution, almandine, aluminum silicate, and quartz. Reactions with micas are less well constrained and their use would add additional uncertainties to the thermodynamic data. The following reactions constitute all the excess-silica end-member dehydration equilibria involving staurolite in the simple FASH system:

3 2H staurolite + 11 quartz
= 4 almandine + 23 sillimanite (or kyanite) + 3 H_2O (1)

3 6H staurolite + 7 quartz
= 2 almandine + 25 sillimanite (or kyanite) + 9 H_2O (2)

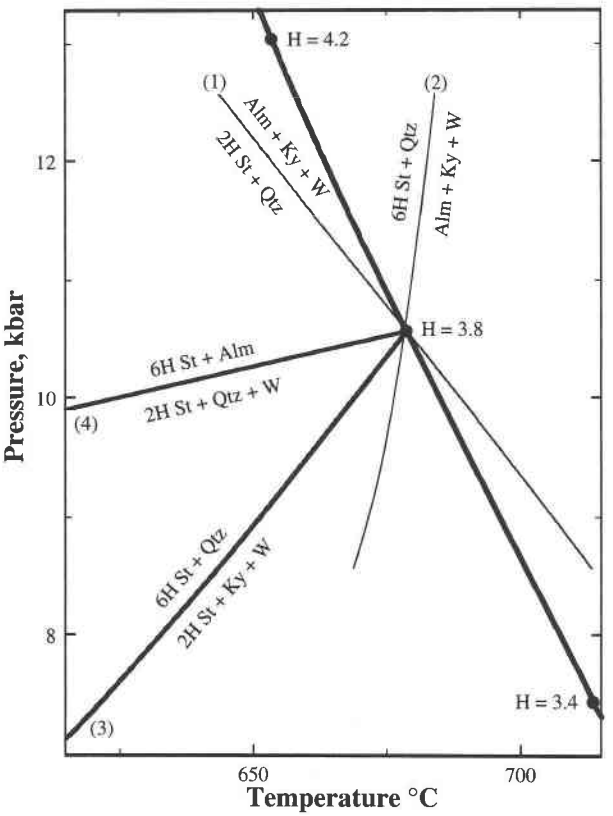

Fig. 2. Illustration of FASH Reactions 1–4 in the kyanite stability field. Reactions 1–4 were calculated using 2H and 6H stoichiometric staurolite end-member thermodynamic data of Table 2 and staurolite H content of 3.8 apfu (formula $H_{3.8}Fe^{2+}_{3.95}Al_{17.80}Fe^{3+}_{0.10}Si_{7.65}O_{48}$). Activity of 2H staurolite is 0.1763; activity of 6H staurolite is 0.00849 (Table 4). Thin curves for Reactions 1 and 2 are staurolite breakdown curves for fixed composition, which are only stable where they cross to define a point on the staurolite breakdown envelope. Medium-thickness curves for Reactions 3 and 4 define *P-T* conditions for 3.8H staurolite with aluminum silicate and almandine, respectively, within the field of staurolite + quartz. As staurolite H content varies, each curve generates a family of curves. Intersections for H = 3.4 and H = 4.2 apfu are also shown, generating the staurolite breakdown envelope.

2 6H staurolite + quartz
= 2H staurolite + 9 sillimanite (or kyanite) + 5 H_2O (3)

23 6H staurolite + 18 almandine
= 25 2H staurolite + 38 quartz + 44 H_2O. (4)

Each of these reactions must be corrected for the activity of 2H or 6H staurolite end-member in the actual staurolite present. Reactions 1 and 2 are breakdown reactions that apply to natural and synthetic staurolite. Reactions 3 and 4 are sliding equilibria between staurolite and aluminum silicate or garnet that must apply within the stability field of staurolite + quartz (Fig. 2). Each point at which any two of these four reactions cross for a given staurolite composition defines a point on the staurolite + quartz

breakdown envelope (Fig. 2). Because all natural and synthetic staurolite crystals are solid solutions of the 2H and 6H end-members, Reactions 1 and 2 are metastable except where they intersect for a given staurolite composition. Whereas Reactions 3 and 4 are stable within the staurolite + quartz stability field, they are metastable outside the staurolite + quartz stability field.

Constraints

For retrieving thermochemical data for 2H and 6H staurolite, there are four unknowns: enthalpy, entropy, H content of equilibrium synthetic staurolite, and possible nonideality of FASH staurolite. We have selected four sets of synthetic and natural constraints, in order of decreasing importance to the problem: (1) The experimental reversals of Richardson (1968), Dutrow and Holdaway (1989), and Dutrow (this report), applied to Reactions 1 and 2 with sillimanite as a product; (2) the experimental reversals of Ganguly (1972) and Rao and Johannes (1979), applied to Reactions 1 and 2 with kyanite as a product; (3) the staurolite + kyanite-bearing rocks of Black Mountain, New Hampshire (5.5 kbar, 495 °C, $a_{H_2O} = 1$; Rumble, 1978), applied to Reaction 3; (4) the staurolite + almandine-bearing rocks of M3 in Maine (3.1 kbar, 540 °C, $a_{H_2O} = 0.86$; Holdaway et al., 1988), applied to Reaction 4. For cases (1) and (2), the H content of synthetic staurolite is not known, whereas for cases (3) and (4), the H content is known (Holdaway et al., 1986a; Dyar et al., 1991).

The experimental constraints were extended by 15 °C in T and 2% in P away from the equilibrium curve to account for experimental error (usually estimated as 5–10 °C), and because (1) many starting staurolite grains were not at their stable composition and may have begun to react to breakdown products before reaching their equilibrium composition, and (2) aluminum silicate starting materials were, in some instances, metastable and might have begun to react to the stable form during the experiment. We estimate that experimental error and metastability effects have about equal weight. These estimated figures apply to all experiments on average, and individual experiments may have a larger error owing to factors discussed below. The plotted positions in Figures 3 and 4 represent each reversal extended by the above amounts in T and P, and thus uncertainties are not shown.

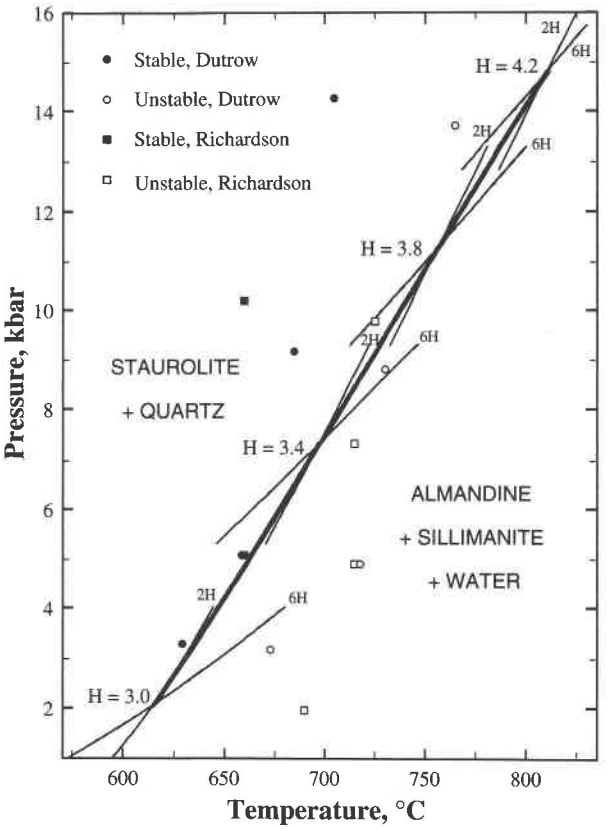

Fig. 3. Calculated and experimental determinations of Reactions 1 and 2 with sillimanite and almandine as products. Solid symbols represent staurolite stability and open symbols represent stability of sillimanite + almandine, each adjusted 15 °C and 2% in P away from the equilibrium curve. Circles represent results of Dutrow and Holdaway (1989) and Dutrow (this report), and squares represent results of Richardson (1968). Fine lines represent segments of Reaction 1 (2H) and Reaction 2 (6H) for the H content given and were calculated using the thermodynamic data of Table 2. These curves intersect to determine points on the overall staurolite breakdown curve shown by the heavy line. Intersections are identified by the H content of staurolite at that P and T in atoms per formula unit. The experimental points and the curve are metastable relative to kyanite and almandine above P and T values of 8 kbar and 707 °C.

Evaluation of experimental constraints

The experimental constraints (Richardson, 1968; Dutrow and Holdaway, 1989; Dutrow, this report; Ganguly, 1972; Rao and Johannes, 1979) are shown for the sillimanite + almandine system (Fig. 3) and for the kyanite + almandine system (Fig. 4). Because of the variable composition of FASH staurolite and the lack of consistency of the experimental results, some general principles were applied to best use these constraints: (1) Most natural starting staurolite (Dutrow and Holdaway, 1989) and synthesized FASH starting staurolite were assumed to have high Fe and low H. Unit-cell measurements suggest that this is the case (Holdaway et al., 1993), and bulk compositions of natural staurolite and mixes for synthesis all had high Fe content. Therefore, to a first approximation, the experimental equilibria pertain to H-poor compositions. (2) All experiments that showed staurolite growth were accepted as valid indications of staurolite stability relative to the alternative assemblage in the experiments, incorporating the previously discussed 15 °C extension away from the equilibrium curve. The reaction products in the starting materials always had stable compositions for the reaction being studied (except where a metastable aluminum silicate was used), whereas the staurolite was not necessarily of equilibrium composition. In some instances, P-T points of apparent staurolite-instability also

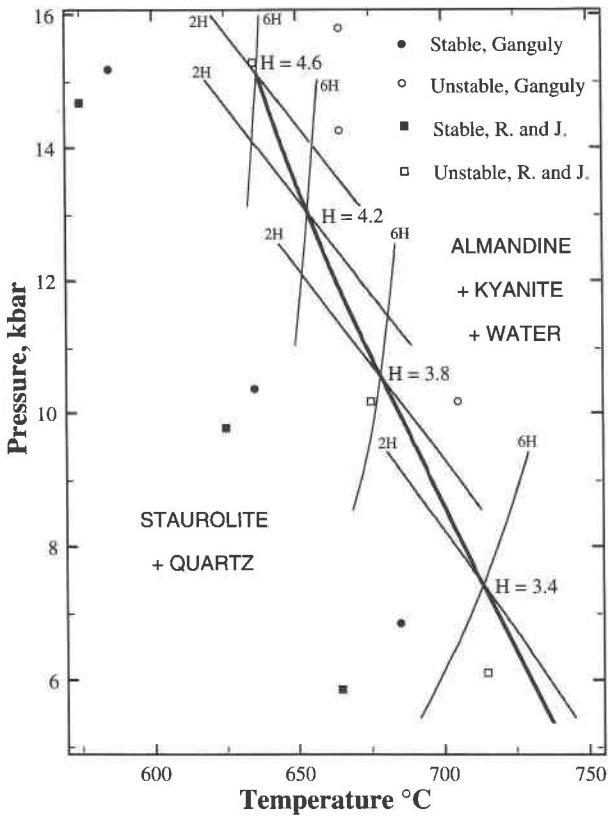

Fig. 4. Calculated and experimental determinations of Reactions 1 and 2 with kyanite and almandine as products. Solid symbols represent staurolite stability and open symbols represent stability of kyanite + almandine, each adjusted 15 °C and 2% in P away from the equilibrium curve. Circles represent the results of Ganguly (1972) and squares represent the results of Rao and Johannes (1979). Fine lines represent segments of Reaction 1 (2H) and Reaction 2 (6H) for the given H content, calculated using thermodynamic data of Table 2. These curves intersect to determine points on the staurolite breakdown envelope shown by the heavy line. Intersections are identified by the H content of staurolite at that P and T in atoms per formula unit. The experimental points and the curve are metastable below P and above T of 8 kbar and 707 °C relative to sillimanite and almandine.

fall in the final staurolite stability field, probably because a highly unstable (H-poor) staurolite composition reacted metastably to the reaction products. Each of these cases also shared one or both of characteristics (3) and (4). (3) P-T points of apparent staurolite instability on the metastable extension of a reaction curve tended to fall inside the final field of staurolite stability (by up to 27 °C in the most extreme case at 765 °C, 13.7 kbar on the sillimanite + almandine curve, Fig. 3). These points might, in part, represent experiments in which the stable aluminum silicate began to grow from staurolite with an unstable H content, giving an apparent indication of staurolite instability relative to the metastable aluminum silicate + almandine (Figs. 3 and 4). (4) The results of Rao and Johannes (1979) on the staurolite to kyanite + almandine reaction consistently indicate staurolite instability 20–30 °C below the experiments of Ganguly (1972). Two Rao and Johannes (1979) reversals are inconsistent with the staurolite to sillimanite + almandine data and with the overall analysis, and fall in the staurolite field (by 8–14 °C, Fig. 4). (5) The experiments of Richardson (1968), Dutrow and Holdaway (1989), and Dutrow (this report) on staurolite to sillimanite + almandine are all consistent with each other, but have P-T slopes significantly greater than that indicated by the corrected calorimetric entropy determined above, suggesting that S of staurolite determined from experiments is substantially lower than the calorimetric value. With this observation in mind, S of 2H and 6H end-member staurolite retrieved from the above constraints was maximized, while disagreement with experimental constraints was minimized.

Procedure

For the calculations used to estimate thermochemical parameters of 2H and 6H FASH staurolite (described below), we used the data base of Berman (1988, updated in 1992 personal communication) for almandine, quartz, and H_2O and the Ge0-Calc program of Brown et al. (1988). In order to account for the most recent thermochemical results of Hemingway et al. (1991), we used the aluminum silicate values of H, S, C_P, and V of Holdaway and Mukhopadhyay (1993). To bring these into agreement with the other minerals of the data base, we subtracted 70 J/mol from H of each polymorph and 0.3 J/(mol·K) from S of each polymorph. These corrections make the aluminum silicate values indistinguishable from those of Berman in two sensitive reactions, the grossular + quartz breakdown and the muscovite + quartz breakdown, and maintain the aluminum silicate P-T diagram of Holdaway and Mukhopadhyay (1993). Use of the Berman aluminum silicate data gives the same result for staurolite H and S. V and C_P data discussed previously (Table 2) were used for 2H and 6H FASH staurolite. The complex set of constraints coupled with three primary variables required a trial and error method in order to approximate the correct H values and thus the correct values of H and S for each end-member. Several trial approaches were used before settling on the most appropriate method. During this procedure it became clear that the general approach outlined below is the most straightforward and gives the best results. Alternative possibilities for H and S are considered in the discussion section.

First, all assumed synthetic-staurolite compositions were activity-corrected for H content as discussed above (Table 4). Natural staurolite that formed at or near conditions of stable reaction to sillimanite + garnet has low H contents (between 3 and 3.4 apfu) regardless of P (Holdaway et al., 1986b; Dyar et al., 1991), suggesting that this curve varies slowly in H content. The experimental data (Fig. 3) indicate a P-T boundary too steep to be consistent with the corrected calorimetric S (Table 3). This problem could

be alleviated by allowing the H content to decrease with increasing P and T along the staurolite + quartz to sillimanite + almandine stability envelope, so that the individual 2H curves in Figure 3 would be flatter than the staurolite + quartz stability envelope. However, our calculations show that Reaction 1 is always steeper than Reaction 2 in the sillimanite field as it releases more moles of H_2O, and thus the H content of staurolite must increase with increasing P along the staurolite + quartz to sillimanite + almandine breakdown curve (Fig. 3). We retrieve S and H of 2H end-member staurolite (Reaction 1) on the basis of the staurolite + quartz to sillimanite + almandine experimental reversals and an assumed H content of 3 apfu. Even though this H content applies to only one point on the stable curve, we consider that the remainder of the experimental data apply reasonably well to a metastable H-poor staurolite on the basis of the composition of the starting staurolite and the fact that at low H content activity of 6H staurolite is very low and Reaction 2 is essentially undefined (Table 4). The starting staurolite of Dutrow and Holdaway (1989) and Dutrow (this report) has 3.27 H apfu. For the 2H end-member, S and H retrieved with the assumption H = 3.27 apfu (the analyzed H content) are 3 J/(mol·K) lower and 1.9 KJ/mol lower, respectively, than the values arrived at by assuming H = 3 apfu. However, the values determined on the basis of H = 3 give a better overall fit to the constraints. Because S is substantially lower than the corrected calorimetrically measured value (Table 3), we maximize S to produce the flattest possible metastable curve consistent with all the reversal data. The stable curve that results from knowledge of 2H and 6H properties (discussed below) is flatter than the experimental curve and flatter than a curve calculated with constant H = 3 apfu. This curve fits all the extended reversals except the two highest P, staurolite-unstable half-reversals on the metastable extension (Richardson, 1968; Dutrow, this report), which deviate by 10 and 27 °C, respectively (Fig. 3). These H and S values (Table 2) are the best possible constraints on the thermodynamic data for 2H staurolite. These data allow calculation of a stable staurolite H content and an H vs. S line for the 6H staurolite end-member for any P-T point at which Equilibria 1 and 2, or 3, or 4 are defined.

Second, if we were to assume a fixed-H staurolite to kyanite + garnet breakdown-curve based on three H apfu using the 2H end-member data determined in the first approach, it would fit the experimental data at the kyanite-sillimanite boundary (about 700 °C, 8 kbar) but would fall at P or T below the Rao and Johannes (1979) and Ganguly (1972) staurolite-stable half-reversals at ~15 kbar, 575 and 585 °C (Fig. 4). Thus, is appears that in experiments at higher P and with starting staurolite synthesized at higher P, the experimental staurolite equilibrated with higher H contents. Given the H and S determined in the first approach, we evaluate the reduced activity of 2H staurolite (Reaction 1) needed to match the staurolite to kyanite + almandine reversals. After considerable experimentation a point on the staurolite to kyanite + almandine curve at 15.3 kbar and 635 °C with H = 4.6 apfu was found to produce the best fit for all the data and to allow for the probability that even at high P the starting staurolite did not equilibrate in H content sufficiently to prevent all metastable breakdown. With that information, we determine an activity of 6H staurolite at the above condition (Table 4). This point is an upper limit in T.

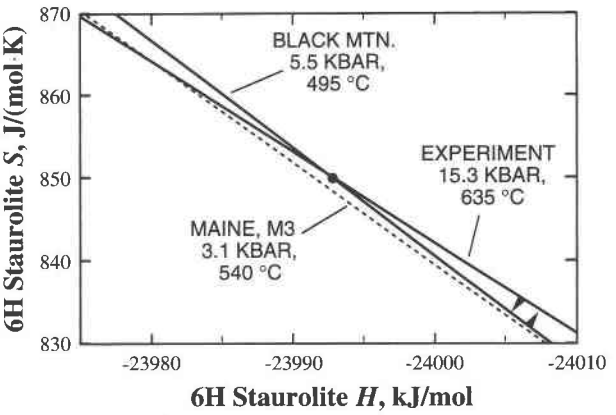

Fig. 5. H-S plots of three constraints on the H and S of stoichiometric 6H staurolite. Arrows identify the field of possible solutions. The dot shows the preferred solution (Table 2), which maximizes S. The constraint from Maine is approximate because of the very low activity of 6H staurolite at those P-T conditions.

Third, because of the absence of information on the H content of stable experimental staurolite, it is not possible to use experimental data alone to constrain S and H of 6H staurolite. If we include well-characterized natural occurrences, there are three distinct P-T points with which to determine H and S of 6H staurolite: (1) with kyanite + almandine at 15.3 kbar, 635 °C, H = 4.6 apfu (Reactions 1 and 2, see above), (2) the Black Mountain, New Hampshire, occurrence at 5.5 kbar, 495 °C, H = 3.99–4.56 apfu (Reaction 3), and (3) the Maine locality at 3.1 kbar, 540 °C, H = 2.97–3.27 apfu (Reaction 4). It appears that case (1) represents a maximum in T because an extended staurolite-breakdown data point of Rao and Johannes (1979) lies at that condition (Fig. 4), case (2) is a minimum in T because formation of staurolite with kyanite in pure H_2O might be expected to occur at T above 500 °C (Richardson, 1968), and case (3) has substantial error. Because of the discrepancy with the calorimetric S, we maximize S. With constraints (1) and (2), we estimate H and S of 6H staurolite (Fig. 5). The values determined for H and S provide reasonable activities of 6H staurolite at all of the above points. The Maine occurrence gives a P-T curve that passes through a T substantially above 540 °C, which was based on garnet + biotite geothermometry (Holdaway et al.,1988). However, this is not a strong constraint because of the small content, large range, and high error of 6H staurolite activity in these specimens (Table 4). The 9 kJ/ion nonideality (Mukhopadhyay et al., 1990) for staurolite T2 gave a better overall fit for the natural occurrences but

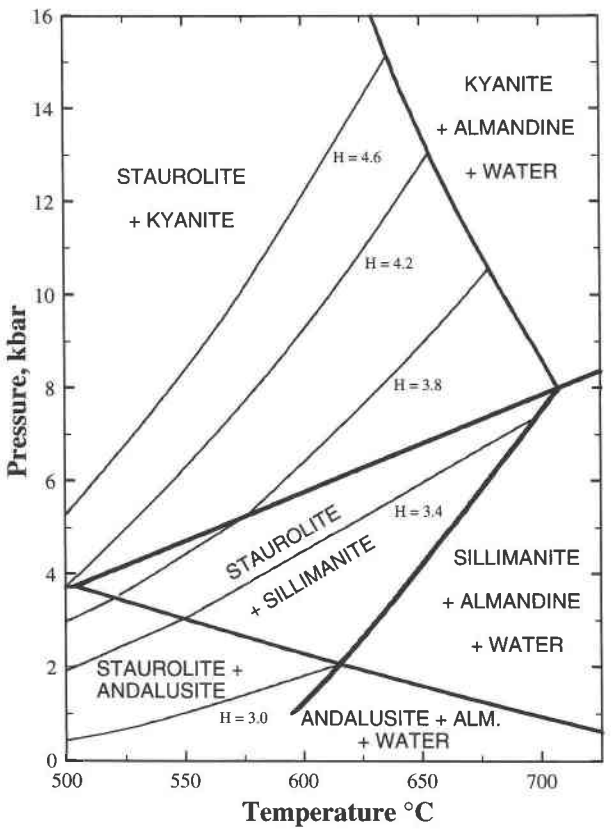

Fig. 6. Contours of H content, in atoms per formula unit, of staurolite with aluminum silicate and quartz, calculated using the thermodynamic data of Table 2 and Reaction 3. These values represent the highest possible H content of staurolite present in a pure FASH system. For natural occurrences, the curves must rise in P (decrease in T) somewhat. For the high-P, low-T region, staurolite should have H in excess of 4.6 apfu.

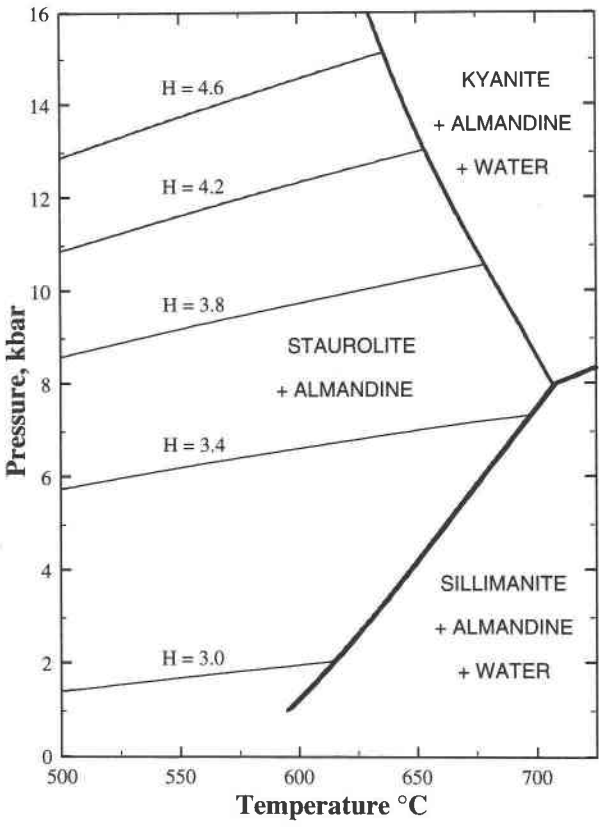

Fig. 7. Contours of H content, in atoms per formula unit, of staurolite with almandine and quartz, calculated using the thermodynamic data of Table 2 and Reaction 4. These values represent the lowest possible H content of staurolite present in a pure FASH system. For natural occurrences, the curves vary in P somewhat.

had negligible effect on the final values of H and S. It should be clear from Figure 5 that more information is available on the relation between H and S of the 6H staurolite end-member than on the specific value of each.

Fourth, the possibility of nonideal solid solution at M4 (Fe^{2+}-H substitution) was tested with plots of activity ratios between P-T points at the highest- and lowest-P constraints (above) for both Reactions 1 and 2 using a variable, symmetrical Margules parameter. These plots showed that nonideality cannot be used to improve the overall fit of the data even if the H content of staurolite is allowed to vary at 15.3 kbar, 635 °C.

Fifth, with these H and S values, we calculate the complete staurolite breakdown curve as a function of variable H content (Reactions 1 and 2; Fig. 2). The stability envelope is determined and compared with individual reversals by calculating points at intervals of 0.2 H pfu (Figs. 3 and 4; an interval of 0.4 H is shown on the diagrams).

Sixth, the staurolite-garnet and the staurolite-aluminum silicate families of curves that occur within the envelope of staurolite + quartz stability (Fig. 2) in the pure FASH system (Reactions 3 and 4; Figs. 6 and 7) are then calculated.

Results

The results are shown diagrammatically in Figures 3, 4, 6, and 7, and the final values of H and S are tabulated in Table 2. It is important to bear in mind that once the best values of H and S are identified for the two end-members, the H contents of all stable FASH staurolite are uniquely determined as a function of P, T, a_{H_2O}, and coexisting garnet or aluminum silicate. Because the retrieved entropies for both 2H and 6H staurolite are substantially below the corrected calorimetric values as determined above (Table 3), the best entropies to use for natural staurolite are those that produce the most satisfactory fit for all of the experimental and natural data (Table 2, Figs. 3 and 4). However, these values must be used in conjunction with the staurolite activity models and H and S values for the other phases used in this study, with the exception that either the Berman (1988, updated in 1992 personal communication) or the modified Holdaway and Mukhopadhyay (1993) aluminum silicate values may be used.

Discussion

Alternative fits

Three alternative possibilities regarding the fit of the experimental data are suggested by Figures 3 and 4: (1) The staurolite + quartz to sillimanite + almandine boundary (Fig. 3) could be made steeper to provide better agreement with all experimental results and also minimize or eliminate the disagreement with the metastable extension reversals. (2) The staurolite + quartz to kyanite + almandine boundary (Fig. 4) could be made flatter and moved to lower P to provide better fit with the Rao and Johannes (1979) reversals. (3) The staurolite H content at 15.3 kbar could be reduced, thus allowing for a flatter staurolite + quartz to kyanite + almandine curve. However, these alternatives would not maximize the consistency among phase equilibrium, calorimetric data, and natural data, as explained below.

With the assumption that the molar volumes, entropies of other participant phases, and H_2O data are reasonably accurate, the calculated staurolite + quartz to sillimanite + almandine curve (Fig. 3) can be steepened by a substantial decrease in the entropy of the 2H staurolite end-member. This requires an accompanying adjustment to the enthalpy. However, such a change would greatly increase the disagreement between the corrected calorimetric and experimentally determined entropy values. The sillimanite + almandine metastable-extension reversals (Fig. 3) seem low in T. This may be in part due to spontaneous crystallization of stable kyanite from staurolite and quartz although no kyanite was identified, but it is primarily due to the fact that the staurolite used in the reactions had low H and high Fe^{2+} for those P-T conditions and probably began to break down metastably before reaching the equilibrium composition. Three of the four half-reversals that disagree with the calculated sillimanite + almandine and kyanite + almandine curves (Figs. 3 and 4) relate to stable staurolite compositions with H = 3.6–4.0 apfu, cf. $\leq$3.1 apfu for synthetic Fe staurolite (Holdaway et al., 1993). The fourth half-reversal (kyanite + almandine in the sillimanite + almandine field, 6.12 kbar, 715 °C, Rao and Johannes, 1979) involves ~3.3 H apfu staurolite and disagrees with the calculated curve by 14 °C. A hypothetical P-T diagram calculated assuming that equilibrium staurolite has a constant three H apfu disagrees with none of the above half-reversals and results in steeper sillimanite + almandine and flatter kyanite + almandine staurolite breakdown curves. Unfortunately, such a diagram disagrees with two important high-P staurolite-stable points for the staurolite + quartz to kyanite + almandine reaction and is almost certainly metastable (Fig. 4).

The staurolite + quartz to kyanite + almandine curve (Fig. 4) could be reduced in slope by increasing 2H-staurolite entropy, but this would further reduce the slope of the sillimanite + almandine curve and disagree with more experimental reversals. The kyanite + almandine curve could be lowered in P by moving the invariant point to lower T, but this would again disagree with experimental constraints for the sillimanite + almandine reaction.

The H content of staurolite at 15.3 kbar (H = 4.6 apfu, Fig. 4) could be reduced to enable a lower T for the high-P end of the kyanite + almandine curve. However, this would cause a misfit with the Black Mountain, New Hampshire, occurrence that would have to be compensated for by further reducing the 6H-staurolite entropy, which is already substantially below the corrected calorimetric value. Staurolite with kyanite at other localities (e.g., Truchas Mountains, New Mexico) also has high H content (Grambling, 1983; Holdaway et al., 1991) and formed at conditions similar to those of the Black Mountain locality.

Sources of error

Error in the determined values of H and S of 2H- and 6H-staurolite end-members is related to three factors: (1) The values of H, S, V, and C_P for garnet, aluminum silicate, quartz, and H_2O, and the values of V and C_P of 2H and 6H staurolite used for the calculations can additively affect the H and S of staurolite. (2) The overall quality of the experimental reversals also has an important effect. The problem is particularly acute for staurolite because of the compositional variation possible in simple FASH staurolite, and because impure staurolite seeds were used as starting materials for some studies. The disagreement between the Ganguly (1972) and Rao and Johannes (1979) reversals may also be affected by additional factors such as inexact calibration or problems in detecting reaction. (3) Perhaps the biggest potential source of error relates to the process of determining activities of hypothetical stoichiometric end-members of staurolite from synthetic and natural compositions. Possible errors could involve nonideal solid solution at one or more sites in the structure, inaccuracy of the activity models, and compositions of staurolite that grew at equilibrium and that may be different from those assumed.

All sources of error may be grouped into two categories: (1) factors that affect all common staurolite crystals at all P-T conditions to about the same extent. These factors may well explain the differences between calculated and retrieved entropies and are not detrimental to using the data of Table 2 for petrogenetic calculations. (2) A second type of error may be attributed to factors that vary in P-T space or with staurolite composition. These factors will adversely affect petrogenetic calculations. The fact that a self-consistent set can be determined on the basis of a reasonable analysis of the existing constraints, and that the 6H-staurolite H and S calculated at high P is reasonably consistent with staurolite compositions at low P suggests that much of the error is of type (1). The fact that the natural occurrences fit slightly better with a nonideal model for non-FASH cations at the T2 site does not provide a sufficient argument to favor the nonideal model.

Because of the complexity of the H and S retrieval problem, it is impossible to accurately assess error for the various quantities. On the basis of experimentation with

the constraints, we estimate errors of ±20 J/(mol·K) and ±20 kJ/mol for S and H of 2H staurolite and ±40 J/(mol·K) and ±40 kJ/mol for S and H of 6H staurolite. In both cases, errors in H and S are strongly correlated. H estimates are believed to be accurate within about 0.3 apfu.

Application to natural and synthetic systems

The present study provides a self-consistent set of thermodynamic data for common staurolite. Because of the complexity of the problem, the assumptions that had to be made, and the difficulties with experimental studies of staurolite, these data need to be carefully tested against natural occurrences. However, they cannot be tested quantitatively until the problem of possible staurolite nonideality at the T2 site is resolved.

The results of this study are generally consistent with calculated P and T of natural occurrences of staurolite and coexisting minerals. Comparison with natural assemblages may be done using Figures 6 and 7, keeping in mind that activities of 2H staurolite, garnet, and H_2O are reduced, relative to the pure FASH system, to a greater extent in nature than the activity of 6H staurolite. The curves in Figure 6 will move to higher P or lower T or both, and those in Figure 7 will move either up or down in P for natural assemblages. Observations include the following: (1) The H content of staurolite is fixed only at or near its breakdown curve. Along that curve, H increases with increasing P from 2.8 to at least 4.6 apfu. Eventually, it might be possible to estimate both P and T from staurolite composition and the coexisting breakdown assemblage. (2) Within the staurolite + quartz stability field, a range of H composition is possible at any given P and T, the maximum H occurring when staurolite coexists with aluminum silicate, and the minimum H occurring when staurolite coexists with Fe-rich almandine. (3) When staurolite occurs with garnet, H content increases mainly with P, and when staurolite coexists with aluminum silicate, H increases with increasing P and decreasing T. (4) Common staurolite that occurs with garnet at 2–5 kbar, has 2.8–3.3 H apfu but the less common occurrences with aluminum silicates show distinctly higher H contents, which are significantly affected by small changes in P and T (Figs. 6 and 7). (5) We can expect to find staurolite with the highest H content at high P and low T (together with kyanite).

The suggestion that synthetic staurolite tends to have low H content (Holdaway et al., 1993) has important ramifications. It is reasonable to expect that synthetic staurolite should be low in H for several reasons: (1) Bulk compositions used for synthesis of Fe^{2+} staurolite are normally Fe:Al:Si = 4:18:7.5 (or 8), meaning that if staurolite begins to grow with higher H and lower Fe^{2+}, garnet will grow and limit the increase in H content. (2) Si and Al may be less soluble and less reactant than Fe and are perhaps less likely to become incorporated into a synthesized phase; the resultant phase is thus enriched in Fe relative to Si and Al. (3) The absence of reported almandine in staurolite synthesis products also suggests that synthetic products could be high in Fe^{2+} and low in H. Synthesis of H-rich staurolite should be possible with long experiment times at high P, low T, and high-H bulk composition buffered with kyanite. The fact that staurolite has variable H and that synthesis seems to produce H-poor staurolite may have affected the chloritoid-staurolite equilibria that have been studied experimentally, especially the chloritoid + quartz to staurolite + kyanite reaction (e.g., Ganguly, 1972). At high P, the experiments might have involved a ~3H staurolite when a staurolite with >4H apfu was stable. A more stable, higher-H staurolite would expand the staurolite field and perhaps steepen or reverse the slopes of the chloritoid-staurolite equilibria.

Acknowledgments

Our research on staurolite crystal chemistry and stability relations has benefited greatly from the recent work of Frank Hawthorne (University of Manitoba) and his colleagues at the University of Pavia, and M. Darby Dyar (West Chester University). We thank the National Science Foundation (grants EAR-8904777 and EAR-9019277 to M.J.H. and B.M.) for research support. B.L.D. thanks the Alexander von Humboldt Foundation and Ruhr Universität, Bochum, Germany, for research support. Constructive reviews were provided by Frank Hawthorne, Rob Berman, L.Y. Aranovich, and an anonymous reviewer.

References cited

Berman, R.G. (1988) Internally-consistent thermodynamic data for minerals in the system Na_2O-K_2O-CaO-MgO-FeO-Fe_2O_3-Al_2O_3-SiO_2-TiO_2-H_2O-CO_2. Journal of Petrology, 29, 445–522.

Brown, T.H., Berman, R.G., and Perkins, E.H. (1988) Ge0-Calc: Software package for calculation and display of pressure-temperature-composition phase diagrams using an IBM or compatible computer. Computers and Geosciences, 14, 279–289.

Dutrow, B.L., and Holdaway, M.J. (1989) Experimental determination of the upper thermal stability of Fe staurolite + quartz at medium pressures. Journal of Petrology, 30, 229–248.

Dutrow, B.L., Holdaway, M.J., and Hinton, R.W. (1986) Lithium in staurolite and its petrologic significance. Contributions to Mineralogy and Petrology, 94, 496–506.

Dyar, M.D., Perry, C.L., Rebbert, C.R., Dutrow, B.L., Holdaway, M.J., and Lang, H.M. (1991) Mössbauer spectroscopy of synthetic and naturally occurring staurolite. American Mineralogist, 76, 27–41.

Eugster, H.P., and Wones, D.R. (1962) Stability relations of the ferruginous biotite, annite. Journal of Petrology, 3, 82–125.

Fyfe, W.S., Turner, F.J., and Verhoogen, J. (1958) Metamorphic reactions and metamorphic facies. Geological Society of America Memoir, 75, 253 p.

Ganguly, J. (1972) Staurolite stability and related parageneses: Constraints from natural and experimental data, and applications to geothermobarometry. Journal of Petrology, 13, 335–365.

Getting, I.C., and Kennedy, G.C. (1970) Effect of pressure on the emf of chromel-alumel and platinum-platinum 10% rhodium thermocouples. Journal of Applied Physics, 41, 4552–4562.

Grambling, J.A. (1983) Reversals in Fe-Mg partitioning between chloritoid and staurolite. American Mineralogist, 68, 373–388.

Hawthorne, F.C., Ugaretti, L., Oberti, R., Caucia, F., and Callegari, A. (1993a) The crystal chemistry of staurolite: I. Crystal structure and site occupancies. Canadian Mineralogist, 31, 551–582.

——— (1993b) The crystal chemistry of staurolite: II. Order-disorder and the monoclonic → orthorhombic phase transition. Canadian Mineralogist, 31, 583–595.

——— (1993c) The crystal chemistry of staurolite: III. Local order and chemical composition. Canadian Mineralogist, 31, 597–616.

Hemingway, B.S., and Robie, R.A. (1984) Heat capacity and thermodynamic functions for gehlenite and staurolite: With comments on the Schottky anomaly in the heat capacity of staurolite. American Mineralogist, 69, 307–318.

Hemingway, B.S., Robie, R.A., Evans, H.T., Jr., and Kerrick, D.M. (1991) Heat capacities and entropies of sillimanite, fibrolite, andalusite, kyanite, and quartz and the Al_2SiO_5 phase diagram. American Mineralogist, 76, 1597–1613.

Henderson, C.M.B., Charnock, J.M., Smith, J.V., and Greaves, G.N. (1993) X-ray absorption spectroscopy of Fe, Mn, Zn, and Ti structural environments in staurolite. American Mineralogist, 78, 477–485.

Holdaway, M.J. (1971) Stability of andalusite and the aluminum silicate phase diagram. American Journal of Science, 271, 97–131.

Holdaway, M.J., and Mukhopadhyay, B. (1993) A reevaluation of the stability relations of andalusite: Thermochemical data and phase diagram for the aluminum silicates. American Mineralogist, 78, 298–315.

Holdaway, M.J., Dutrow, B.L., Borthwick, J., Shore, P., Harmon, R.S., and Hinton, R.W. (1986a) H content of staurolite as determined by H extraction line and ion microprobe. American Mineralogist, 71, 1135–1141.

Holdaway, M.J., Dutrow, B.L., and Shore, P. (1986b) A model for the crystal chemistry of staurolite. American Mineralogist, 71, 1142–1159.

Holdaway, M.J., Dutrow, B.L., and Hinton, R.W. (1988) Devonian and Carboniferous metamorphism in west-central Maine: The muscovite-almandine geobarometer and the staurolite problem revisited. American Mineralogist, 73, 20–47.

Holdaway, M.J., Mukhopadhyay, B., Dyar, M.D., Dutrow, B.L., Rumble, D., III, and Grambling, J.A. (1991) A new perspective on staurolite crystal chemistry: Use of stoichiometric and chemical end-members for a mole fraction model. American Mineralogist, 76, 1910–1919.

Holdaway, M.J., Gunst, R.F., Mukhopadhyay, B., and Dyar, M.D. (1993) Staurolite end-member molar volumes determined from unit-cell measurements of natural specimens. American Mineralogist, 78, 56–67.

Lonker, S.W. (1983) The hydroxyl content of staurolite. Contributions to Mineralogy and Petrology, 84, 36–42.

Mukhopadhyay, B., Holdaway, M.J., Gunst, R., and Dyar, M.D. (1990) Endmember thermochemical parameters and mixing properties of 3-hydrogen Fe-staurolite. Geological Society of America Abstracts with Programs, 22, 349.

Pigage, L.C., and Greenwood, H.J. (1982) Internally consistent estimates of pressure and temperature: The staurolite problem. American Journal of Science, 282, 943–969.

Rao, B.B., and Johannes, W. (1979) Further data on the stability of staurolite + quartz and related assemblages. Neues Jahrbuch für Mineralogie Monatshefte, 437–447.

Richardson, S.W. (1968) Staurolite stability in a part of the system Fe-Al-Si-O-H. Journal of Petrology, 9, 467–488.

Rumble, D., III (1978) Mineralogy, petrology, and oxygen isotope geochemistry of the Clough Formation, Black Mountain, western New Hampshire, U.S.A. Journal of Petrology, 19, 317–340.

Spear, F.S. (1993) Metamorphic phase equilibria and pressure-temperature-time paths. In Mineralogical Society of America Monograph, 799 p. Mineralogical Society of America, Washington, DC.

Yardley, B.W.D. (1981) A note on the composition and stability of Fe-staurolite. Neues Jahrbuch für Mineralogie Monatshefte, 127–132.

Zen, E-an (1981) Metamorphic mineral assemblages of slightly calcic pelitic rocks in and around the Taconic allochthon, southwestern Massachusetts and adjacent Connecticut and New York. U.S. Geological Survey Professional Paper, 1113.

Manuscript received September 22, 1993
Manuscript accepted January 20, 1995